Hindawi Publishing Corporation
Advances in Meteorology
Volume 2016, Article ID 5836070, 11 pages
http://dx.doi.org/10.1155/2016/5836070

Research Article

A Modeling Study of Impact of Emission Control Strategies on $PM_{2.5}$ Reductions in Zhongshan, China, Using WRF-CMAQ

Jianhua Mai,[1,2] Tao Deng,[2] Lingling Yu,[3] Xuejiao Deng,[2] Haobo Tan,[2] Shiqiang Wang,[4] and Xiantong Liu[2]

[1] *Zhongshan Meteorological Service, Zhongshan 528400, China*
[2] *Institute of Tropical and Marine Meteorology/Guangdong Provincial Key Laboratory of Regional Numerical Weather Prediction, China Meteorological Administration, Guangzhou 510080, China*
[3] *Guangdong Meteorological Observatory, Guangzhou 510080, China*
[4] *Zhuhai Meteorological Service, Zhuhai 519000, China*

Correspondence should be addressed to Tao Deng; tdeng@grmc.gov.cn

Received 13 November 2015; Accepted 17 March 2016

Academic Editor: Renate Forkel

A WRF-CMAQ modeling system is used to assess the impact of emission control strategies and weather conditions on haze pollution in Zhongshan, Guangdong Province, China. One-month simulations for January 2014 are completed and evaluated with the observational data. The simulations show reasonable agreement with the observations. Several sensitivity studies are completed to quantify the percentage contributions of local emissions versus regional emissions to the $PM_{2.5}$ concentrations under different weather conditions. The results indicate that the contributions from local emission is higher than those of the emissions from regional transport when there is no intrusion of cold front (i.e., 58% contribution from local emission versus 42% contribution from the regional transport). The contribution of regional transport is increased to 76% when a strong cold front appears. Furthermore, the sensitivity study demonstrates that $PM_{2.5}$ concentrations on the first, second, and third days are reduced by 47%, 52%, and 58%, respectively, after the local emissions are turned off when there is no intrusion of cold front. Finally, a case study shows that industrial, residential, and mobile emissions account for 24%, 22%, and 15% of the change of $PM_{2.5}$, respectively, during a heavy haze pollution event in Zhongshan.

1. Introduction

With rapid development of urbanization and industrialization, anthropogenic emissions have been increased significantly over the past several decades [1]. Haze has become a very serious air pollution problem in the Pearl River Delta (PRD) region and other regions in China [2]. High ambient levels of particulate matters with diameters less than 2.5 micrometer ($PM_{2.5}$) can reduce visibility significantly, attenuate solar radiation, and pose harmful impact on human health [3, 4]. The observational data show that the number of haze episode days (the episode day is defined when daily mean $PM_{2.5}$ concentrations exceed 75 $\mu g/m^3$, the National Ambient Air Quality Standard for $PM_{2.5}$ in China (NAAQSC) for $PM_{2.5}$) was over 100 in the PRD during the past decade [5]. The haze pollution has received a great concern from the governments and general public. Thus, understanding the relative contribution of local emissions and regional transport is extremely important to reduce $PM_{2.5}$ concentrations.

Many research efforts have been devoted to investigating chemical composition characteristics of $PM_{2.5}$ and impact of weather systems and other meteorological fields on haze over the past several decades [6–13]. The monitoring data show that carbonaceous and inorganic secondary aerosols are the two major contributors to $PM_{2.5}$ in the PRD [14]. Previous studies have pointed out that emissions outside of the PRD exert an important impact on $PM_{2.5}$ in the PRD [15]. But they did not quantify the relative contributions. With the rapid development of computer technologies, numerical air quality models have become very useful tools for air pollution studies [16]. The Hybrid Single Particle Lagrangian Integrated Trajectory (HYSPLIT) model was first

used to track the sources of air masses that have important impact on haze pollution events [17, 18]. Later, several more complicated numerical models were utilized to investigate air pollution events [19, 20]. For example, the Community Multiscale Air Quality (CMAQ) model has been widely used to study pollution events in the PRD [21–25]. These studies have shown that haze pollution severity in the PRD is mainly controlled by anthropogenic emissions with strong spatial variation. They also pointed out that weather conditions are the key to trigger the haze pollution events [26]. However, very few studies have identified the relative contributions of local emissions and regional transport to $PM_{2.5}$ concentrations under different weather conditions in the PRD region. Thus, accurate quantification of relative contributions of local emissions and regional transport to $PM_{2.5}$ is essential to formulate effective emission control strategies.

Zhongshan, an important part of the PRD region, suffers from similar severe haze pollutions. Study of impact of weather conditions and emissions control strategies on haze events is relatively lacking in Zhongshan as compared to other cities in the region [27]. 16 haze episode days was observed in January 2014. The offline coupling system of Weather Research and Forecast (WRF) with CMAQ is used to evaluate the impact of weather conditions and to quantify the relative contribution of local emission and regional transport to the haze events in Zhongshan. Sensitivity studies are designed to assess the contributions of different anthropogenic emissions such as industrial, residential, and mobile sources to the changes of $PM_{2.5}$ during a heavy haze event. The study is aimed at providing scientific evidences for local policy-makers to develop more effective emission control measures.

2. Methods

2.1. Descriptions of Models and Simulation Configurations. The WRF model (version 3.3.1) [28] is used to provide meteorological inputs to drive CMAQ (version 5.0.2). The National Center for Environmental Prediction (NCEP) Final Operational Global Analysis data with spatial resolution of $1^\circ \times 1^\circ$ and time interval of 6 hr are used to generate initial and boundary conditions for the WRF simulations. The WRF single-moment 6-class microphysics scheme (WSM6) [29] and MM5 similarity surface layer scheme [30] are used in the WRF runs. The Noah land-surface model [31] and Yonsei University Boundary layer scheme (YSU) [32] are also utilized in the WRF simulations. The CMAQ model is used to simulate different physical and chemical processes of gaseous pollutants and particulate matter (PM) compositions. The carbon bond (CB05) gas-phase chemical mechanism [33] and the AERO5 module [34] are utilized in the simulations. The detailed model configuration options are listed in Table 1.

Figure 1(a) shows the modeling domains. Two-nested domains are used in WRF and CMAQ simulations with 31 vertical levels. The horizontal resolutions are 27 km and 9 km in coarse and inner domains, respectively. The exterior domain of CMAQ model covers most regions of China and the interior domain covers the whole Guangdong Province. The locations of major cities in the PRD are given in Figure 1(b). The simulations are conducted for the periods from 08:00 LST (Local Standard Time) on 25 December 2013 to 08:00 LST on 1 February 2014. The default boundary conditions are used for the CMAQ simulations in the CMAQ exterior domain. The first seven-day simulations are used as the spin-up runs to minimize the influence of default initial conditions.

Table 1: A summary of configurations used in the WRF-CMAQ simulations.

Physics and chemistry	Parameterization schemes
Microphysics	WSM6
Surface layer	MM5 similarity surface layer
Land-surface model	Noah
Boundary layer	YSU
Chemical gas-phase mechanism	CB05
Aerosol module	AERO5

Emissions are one of the most important factors to the air quality simulations. Many other studies have been devoted to improve the emission inventory in China [35, 36]. This study uses the Multiresolution Emission Inventories for China (MEIC) version 2010, originally developed by Tsinghua University, China [37], and represents the latest emission inventory data in China. The emissions of MEIC are divided into five categories. They include the emissions from power plants, industry, agriculture, transportation, and residential areas. The monthly mean emissions of gas pollutants such as SO_2, NO_x, CO, and NH_3, aerosol chemical compositions such as sulfate, nitrate, ammonium, black carbon, and organic carbon, and other substances are used in the simulations. Given the resolution of $0.25^\circ \times 0.25^\circ$ for original emissions, the emission data are linearly interpolated into the inner domain and the curvature effect of the earth is taken into account during the interpolation.

Figure 2 shows the spatial distributions of annual mean emissions of NO_x, SO_2, CO, and $PM_{2.5}$ in the inner domain of CMAQ. It is found that major cities are the dominant sources of different emissions. For example, more than 500×10^6 moles of NO_x and 100×10^3 kg of $PM_{2.5}$ are emitted from grids of Guangzhou, Foshan, and Shenzhen each year in the model. The temporal variations of the MEIC data are given by Zheng et al. [38].

2.2. Contributions of Emissions from Different Regions. To quantify the relative contributions of local and different regional emissions, the emissions are treated as four different cases: local emissions from Zhongshan, emissions from other cities in the PRD, emissions outside of Guangdong Province, and emissions from other cities in Guangdong Province. Four scenarios are designed to evaluate the contributions of different emissions to $PM_{2.5}$ concentrations by turning off individual emission. The details of different emissions are shown in Figure 1(b) (emissions from outside of Guangdong Province are not showed in the figure) and Table 2. The first

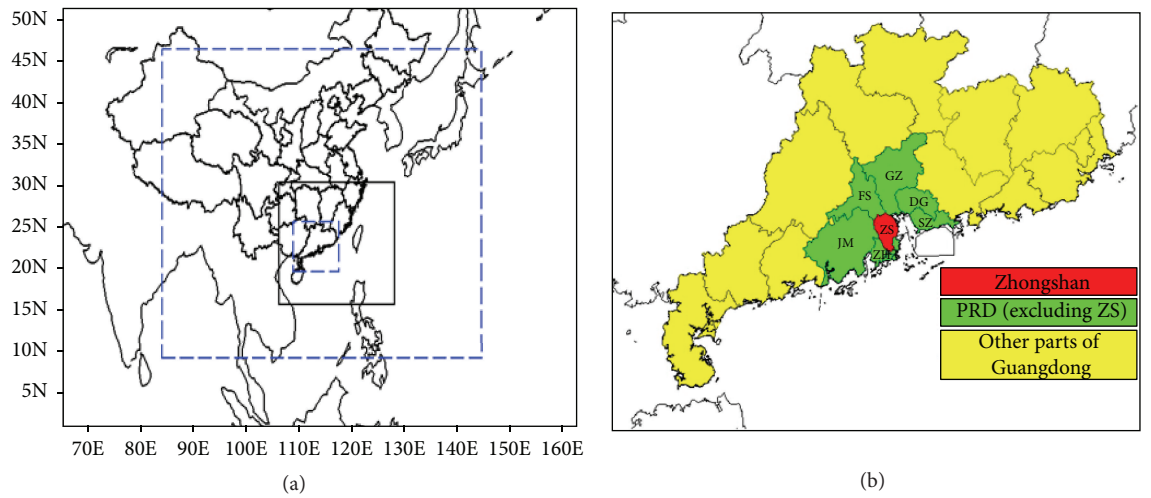

Figure 1: (a) Two-nested modeling domains for WRF (black solid boxes) and CMAQ (blue dashed boxes) models. (b) The inner CMAQ domain with three emission source regions and the major cities in the PRD region (cities in the PRD: Zhongshan (ZS), Guangzhou (GZ), Foshan (FS), Jiangmen (JM), Zhuhai (ZH), Dongguan (DG), and Shenzhen (SZ)).

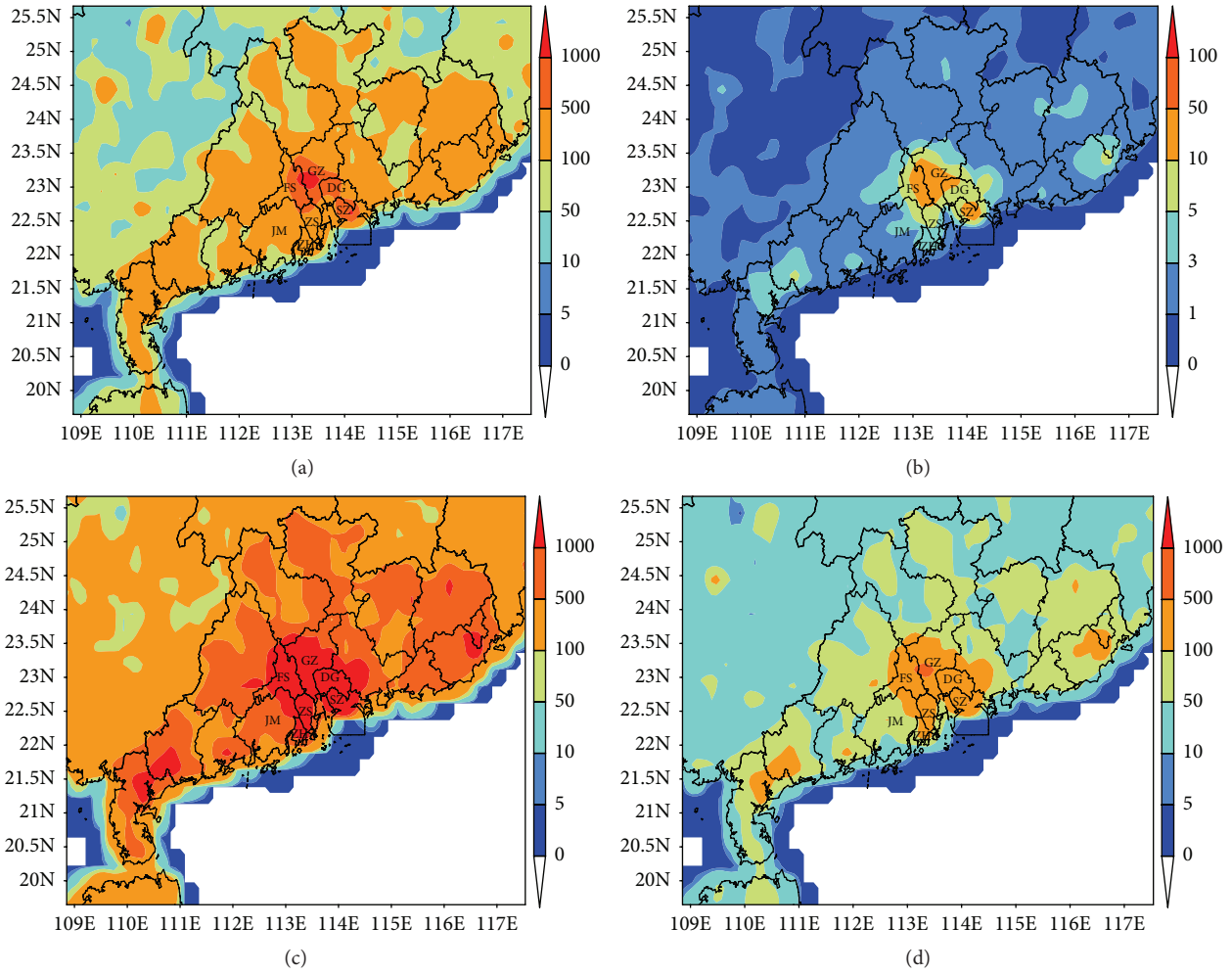

Figure 2: Annual emissions of (a) NO_x, (b) SO_2, (c) CO (unit: $\times 10^6$ mol/year/grid), and (d) $PM_{2.5}$ (unit: $\times 10^3$ kg/year/grid) in the inner domain of CMAQ (cities in the PRD: Zhongshan (ZS), Guangzhou (GZ), Foshan (FS), Jiangmen (JM), Zhuhai (ZH), Dongguan (DG), and Shenzhen (SZ)).

Table 2: A summary of experiment simulations.

Experiment	Regions where emissions were turned off
Test_ctr	None
Test_zs	Zhongshan
Test_prd	PRD (excluding Zhongshan)
Test_gd	Outside of Guangdong Province

scenario: Test_ctr is the control simulation representing the benchmark with original emissions. The second scenario: Test_zs represents the case when the local emissions of Zhongshan are turned off. The third scenario: Test_prd is the case when the emissions of other cities in the PRD are turned off. This case is used to evaluate the influence of emissions from surrounding regions of Zhongshan. The last scenario: Test_gd is the case when the emissions from outside of Guangdong Province are turned off. The contribution of each region can be calculated by using the following formulas:

$$C_x = C_{\text{ctr}} - C_{x,0},$$
$$P_x = \frac{C_x}{C_{\text{ctr}}}, \quad (1)$$

where C_{ctr} represents the $PM_{2.5}$ concentrations as the benchmark; $C_{x,0}$ is the $PM_{2.5}$ concentrations when the emissions of region x are set to zero; C_x represents the difference of $PM_{2.5}$ concentrations between emissions which are turned on and off in region x; P_x represents the contribution of emissions from region x. The similar method has been used by other air quality modeling studies of 2008 Beijing Olympic Game [39, 40].

3. Evaluation of Meteorological and Air Quality Model Simulations

3.1. Evaluation of Meteorological Simulations. Meteorological inputs are important for air quality modeling study. Surface observational data at the sites of Zhongshan (113.35°E, 22.53°N), Guangzhou (113.33°E, 23.17°N), and Zhuhai (113.57°E, 22.28°N) are used to verify the WRF simulations. Figure 3 shows the comparisons of WRF simulated daily mean 2m temperature, daily mean relative humidity, 24-hour surface pressure difference, and daily mean wind speed with observational data in January 2014. Here, the surface pressure difference denotes the one between the current day and one day before. The positive difference in winter indicates an intrusion of a cold front. It is seen from Figure 3 that the simulated 2m temperature at the three sites is slightly higher than the observed temperature but the temporal variation patterns are matched with the observations quite well. The relative humidity is a little lower than the observed value. The simulated 24-hour surface pressure difference shows excellent agreement with the observations at these three sites. It is found that six evident cooling periods were associated with the cold front activities, namely, 3–5, 8-9, 12-13, 18-19, 21-22, and 26-27 January (the shaded areas in Figure 3). The wind speeds are overpredicted for most of the study periods, especially for the days with the substantial impact from cold fronts (e.g., 8, 18, and 21 January). But the tendency of daily variations fits the observational value well. Overall, the simulations show that the WRF model is able to provide reasonable meteorological inputs for driving air quality modeling in January 2014.

3.2. Evaluation of CMAQ Model Results. Figure 4 shows the time series comparison of $PM_{2.5}$ concentrations and visibility between the model simulations and observations in Zhongshan in January 2014. The hourly air quality observational data are used here. Currently, there are four observational sites in Zhongshan. Owing to the sites being close to each other, the averaged $PM_{2.5}$ simulations are compared with the averaged observations at these four sites. As shown in Figure 4, overall, the model is able to capture the general temporal variation patterns of $PM_{2.5}$ concentrations at the observational sites. However, the model underpredicts most peak values of $PM_{2.5}$ substantially and overpredicts the $PM_{2.5}$ at some other time. The simulation biases are highly related to the uncertainties of emissions and the WRF and CMAQ simulations. The underpredictions of $PM_{2.5}$ are usually associated with the overprediction of wind speed when there is no intrusion of cold front. 5 January is an example of that. A large amount of air pollutants is transported to the downwind areas when a strong cold front moves southward. The pollutants can be transported over a longer distance when the cold front is strong enough. But the minor impact of extraneous transport on local $PM_{2.5}$ concentrations is found if the simulated cold front is weaker than the observation (i.e., the simulated 24-hour surface pressure difference is less than observation). A typical example is illustrated on 12 January. Figure 4 also shows large impact of uncertainty of emissions on $PM_{2.5}$ predictions. The anthropogenic emissions are much lower than the normal level during the 3-day periods before Chinese New Year's Eve (i.e., 28–30 January). The change has not been included in the current emission inventory. As a result, the simulated $PM_{2.5}$ concentrations are much higher than the observations during those three days. On the other hand, the model is not able to capture the $PM_{2.5}$ peak value (236 $\mu g/m^3$) on the Chinese New Year's Eve (i.e., 31 January). This is mainly because the firework emissions are not included in the current emission inventory used in the simulations.

Figure 4(b) shows a comparison of simulated and observed visibility. It is noticed that overpredictions of visibility are quite substantial during several days, especially for the days when there is no intrusion of cold front. This is partly because the $PM_{2.5}$ concentrations are usually underpredicted during these days (see 5 January as an example). It is recalled that humidity is another important factor to the change of visibility (see the formula in [41]). The uncertainties of humidity simulation may cause the bias of visibility calculation based on the CMAQ simulations.

Several statistical metrics are used to evaluate the model performance. They include mean bias (MB), mean absolute

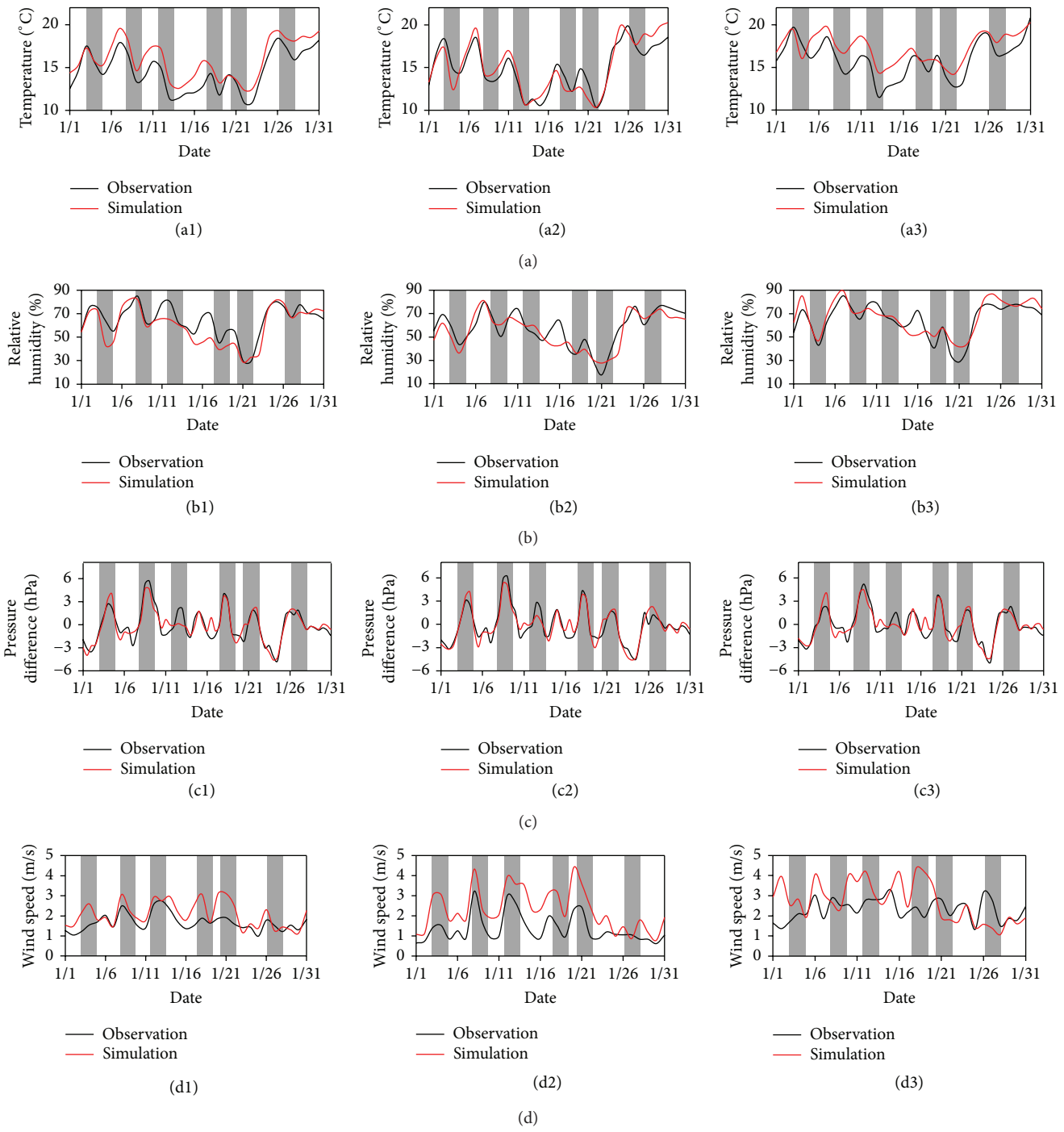

FIGURE 3: Comparison of simulated (a) daily mean 2m temperature, (b) daily mean relative humidity, (c) 24-hour surface pressure difference, and (d) daily mean wind speed with the observations (1, 2, and 3 of each panel represent Zhongshan, Guangzhou, and Zhuhai station, resp. The shaded areas represent the days with cold front intrusion).

error (MAE), root mean square error (RMSE), mean normalized bias (MNB), normalized mean bias (NMB), and correlation coefficient (COR). They are defined as follows:

$$\mathrm{MB} = \frac{1}{n}\sum_{i=1}^{n}\left(\mathrm{Sim}\,(i) - \mathrm{Obs}\,(i)\right),$$

$$\mathrm{MAE} = \frac{1}{n}\sum_{i=1}^{n}\left|\mathrm{Sim}\,(i) - \mathrm{Obs}\,(i)\right|,$$

$$\mathrm{RMSE} = \left[\frac{1}{n}\sum_{i=1}^{n}\left(\mathrm{Sim}\,(i) - \mathrm{Obs}\,(i)\right)^2\right]^{1/2},$$

$$\mathrm{MNB} = \frac{1}{n}\sum_{i=1}^{n}\left(\frac{\mathrm{Sim}\,(i) - \mathrm{Obs}\,(i)}{\mathrm{Obs}\,(i)}\right),$$

$$\mathrm{NMB} = \frac{\sum_{i=1}^{n}\left(\mathrm{Sim}\,(i) - \mathrm{Obs}\,(i)\right)}{\sum_{i=1}^{n}\mathrm{Obs}\,(i)},$$

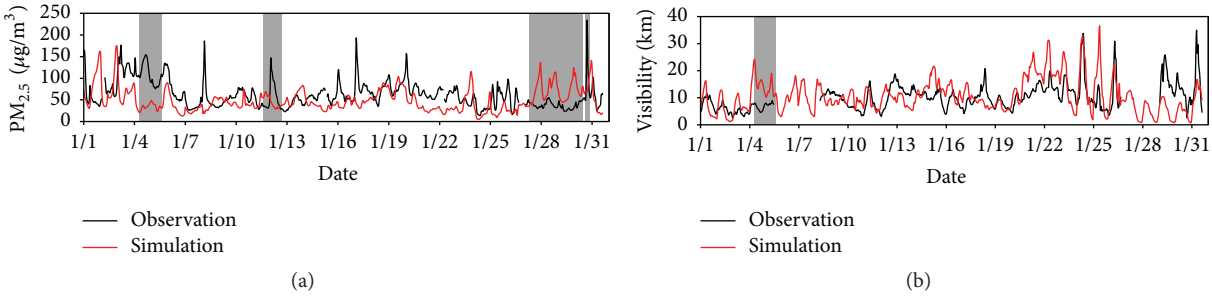

Figure 4: Comparison of simulated (a) $PM_{2.5}$ concentrations and (b) visibility with observations (the discontinuities are due to the missing observational data. The shaded areas in panel (a) denote 5, 12, 28–30, and 31 January mentioned in Section 3.2. The shaded area in panel (b) denotes 5 January).

$$\mathrm{COR} = \frac{\sum_{i=1}^{n}\left[\left(\mathrm{Sim}\,(i)-\overline{\mathrm{Sim}}\right)\left(\mathrm{Obs}\,(i)-\overline{\mathrm{Obs}}\right)\right]}{\sqrt{\sum_{i=1}^{n}\left(\mathrm{Sim}\,(i)-\overline{\mathrm{Sim}}\right)^{2}}\times\sqrt{\sum_{i=1}^{n}\left(\mathrm{Obs}\,(i)-\overline{\mathrm{Obs}}\right)^{2}}}, \quad (2)$$

where Sim and Obs represent simulated and observed values, respectively, and n is the number of the values. The evaluation statistics of the CMAQ performance on $PM_{2.5}$ and visibility are shown in Table 3. It is found that the simulated $PM_{2.5}$ concentrations are lower than the observations and the simulated visibility is slightly overpredicted. And the correlation coefficient is 0.43 and 0.39 for $PM_{2.5}$ concentrations and visibility, respectively. Overall, the statistical calculations indicate that the simulation shows reasonable agreement with the observations.

Table 3: The evaluation statistics of CMAQ performance on $PM_{2.5}$ ($\mu g/m^3$) and visibility (km).

	MB	MAE	RMSE	MNB	NMB	COR
$PM_{2.5}$	−13.4	32.1	29.2	−4.0%	−21.4%	0.43
Visibility	0.8	4.9	5.6	8.2%	20.2%	0.39

4. Sensitivity Analysis

4.1. Contributions of Different Regional Emissions. Figure 5(a) shows the spatial distribution of monthly mean simulated $PM_{2.5}$ concentrations. An area with relatively high concentrations of $PM_{2.5}$ is found in the middle of Foshan, where the monthly mean $PM_{2.5}$ concentrations exceed 60 $\mu g/m^3$. $PM_{2.5}$ concentrations in the northwest of Zhongshan are 50–55 $\mu g/m^3$, but only 35–40 $\mu g/m^3$ is found in the southern part. $PM_{2.5}$ from northwestern to southeastern of Zhongshan is gradually reduced. Figure 5(b) illustrates the percentage contribution of local emissions in Zhongshan. The contribution reaches 45% in the northwest of Zhongshan but reduces to 30–35% in the southern area. The downwind areas of Zhongshan, including parts of Jiangmen and Zhuhai, are also affected by the emissions from Zhongshan. Figure 5(c) shows the percentage contributions of the emissions in other cities of the PRD (see Figure 1(b)). Evidently, the contribution in the middle and southeast of Foshan exceeds 60%. Contributions in southern Guangzhou, western Dongguan and Shenzhen, and eastern Jiangmen are higher than 50%. These emissions contribute 35–45% of $PM_{2.5}$ in northern and 25–30% in southern Zhongshan. In addition, the emissions from outside of Guangdong Province have important impact on the PRD region (see Figure 5(d)). These emissions contribute relatively less over the southeast of Foshan, but the contribution gradually increases in other parts of the PRD. As to Zhongshan, the emissions from outside of Guangdong Province contribute about 25% in the northern part and increase to 35–40% in southern areas. Therefore, the emissions of local Zhongshan, other cities in the PRD, and outside of Guangdong Province are all important to $PM_{2.5}$ concentrations in Zhongshan.

4.2. Regional Transport with Different Weather Conditions. The weather conditions play an important role in regional air pollutant transport. Figure 6 shows the percentage contributions from different emission source regions under different weather conditions in Zhongshan. Haze pollution is mainly caused by low wind speeds and stable atmospheric boundary layer condition when there is no intrusion of cold front (i.e., 24-hour surface pressure difference is negative). Meanwhile, such weather conditions are not beneficial to long-distance transport of air pollutants. So the contributions from local sources, other cities in the PRD, outside of Guangdong Province, and other emissions in Guangdong Province to $PM_{2.5}$ in Zhongshan are 58%, 27%, 13%, and 2%, respectively. A large amount of nonlocal pollutants from outside of Guangdong Province is transported to the PRD region when a strong cold front (24-hour surface pressure difference is more than 3 hPa) moves southwards. The contribution of the emissions from outside of Guangdong Province is increased to 52% in this case, followed by local emissions of Zhongshan (24%) and other cities in the PRD (20%). The air pollutants are mainly controlled by short-distance transport when a weak cold front (24-hour surface pressure difference is about 0–3 hPa) appears. The contribution of emissions from other cities in the PRD increases to 42%, followed by

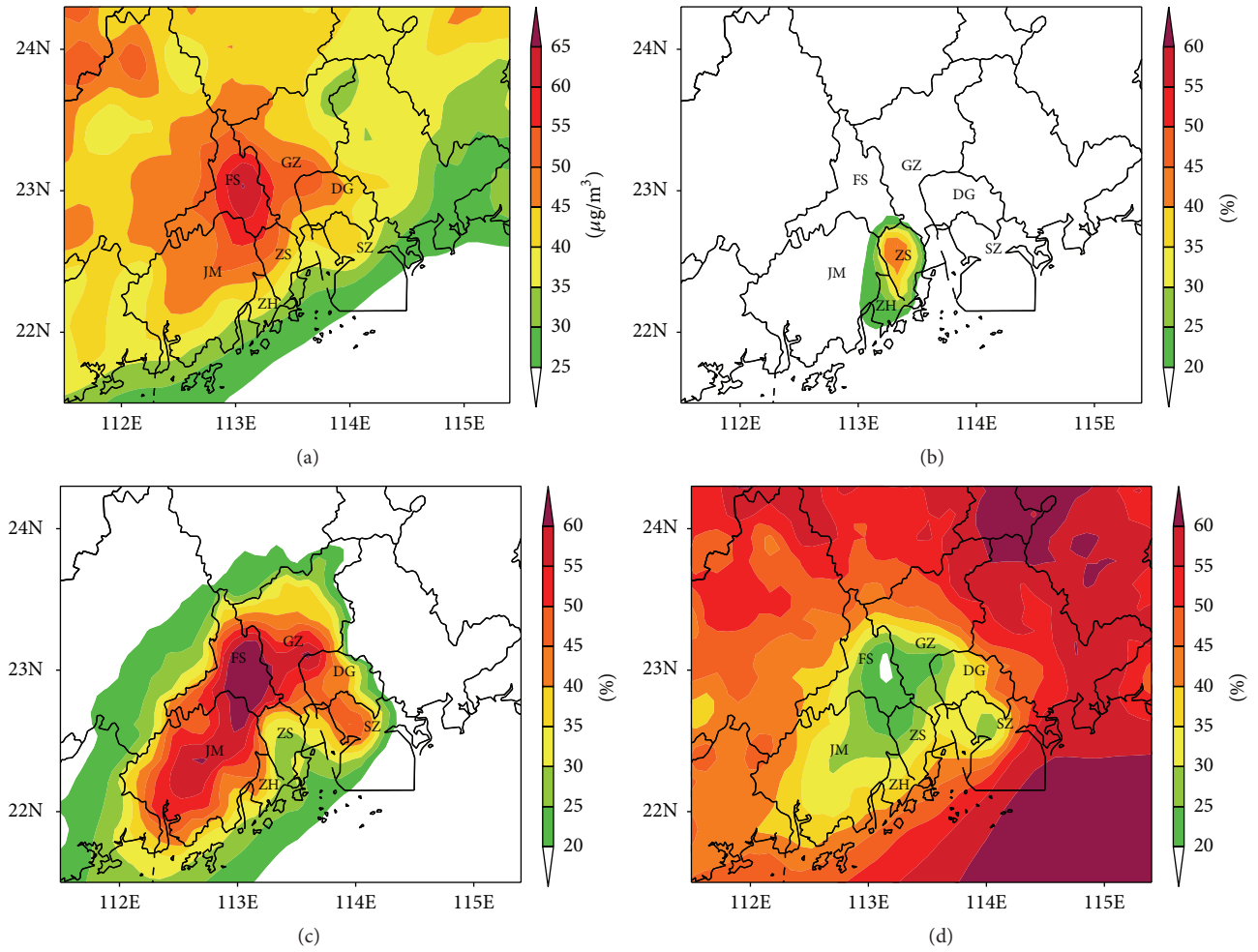

Figure 5: (a) Spatial distribution of simulated monthly mean $PM_{2.5}$ concentrations, (b) percentage contributions of local emissions in Zhongshan, (c) percentage contributions of emissions from other cities in the PRD, and (d) percentage contributions of emissions from outside of Guangdong Province.

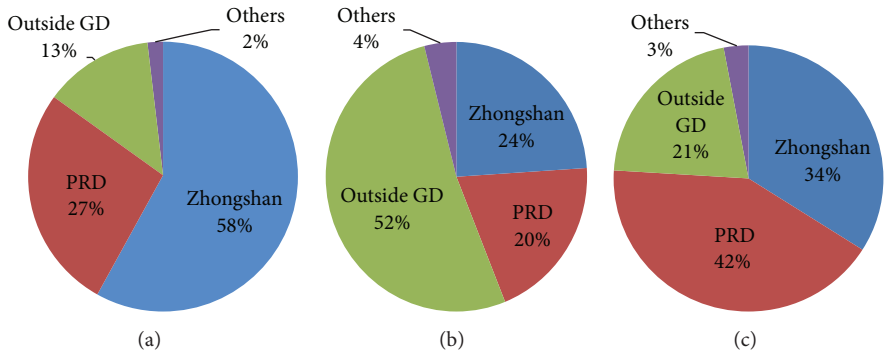

Figure 6: Percentage contributions of the emissions from different regions to the simulated $PM_{2.5}$ in Zhongshan under (a) no cold front, (b) strong cold front, and (c) weak cold front case.

local emissions of Zhongshan (34%) and the emissions from outside of Guangdong Province (21%).

According to the analysis presented above, it is found that emissions outside of Guangdong Province contribute the most changes of local $PM_{2.5}$ concentrations in Zhongshan with intrusions of strong cold front in the PRD region. Figure 7 shows the impact of regional transport on $PM_{2.5}$ in Zhongshan during 8-9 January. It is found that the most polluted areas were located in Hunan Province in the morning of 8 January. As the cold front moved southwards, the aerosol

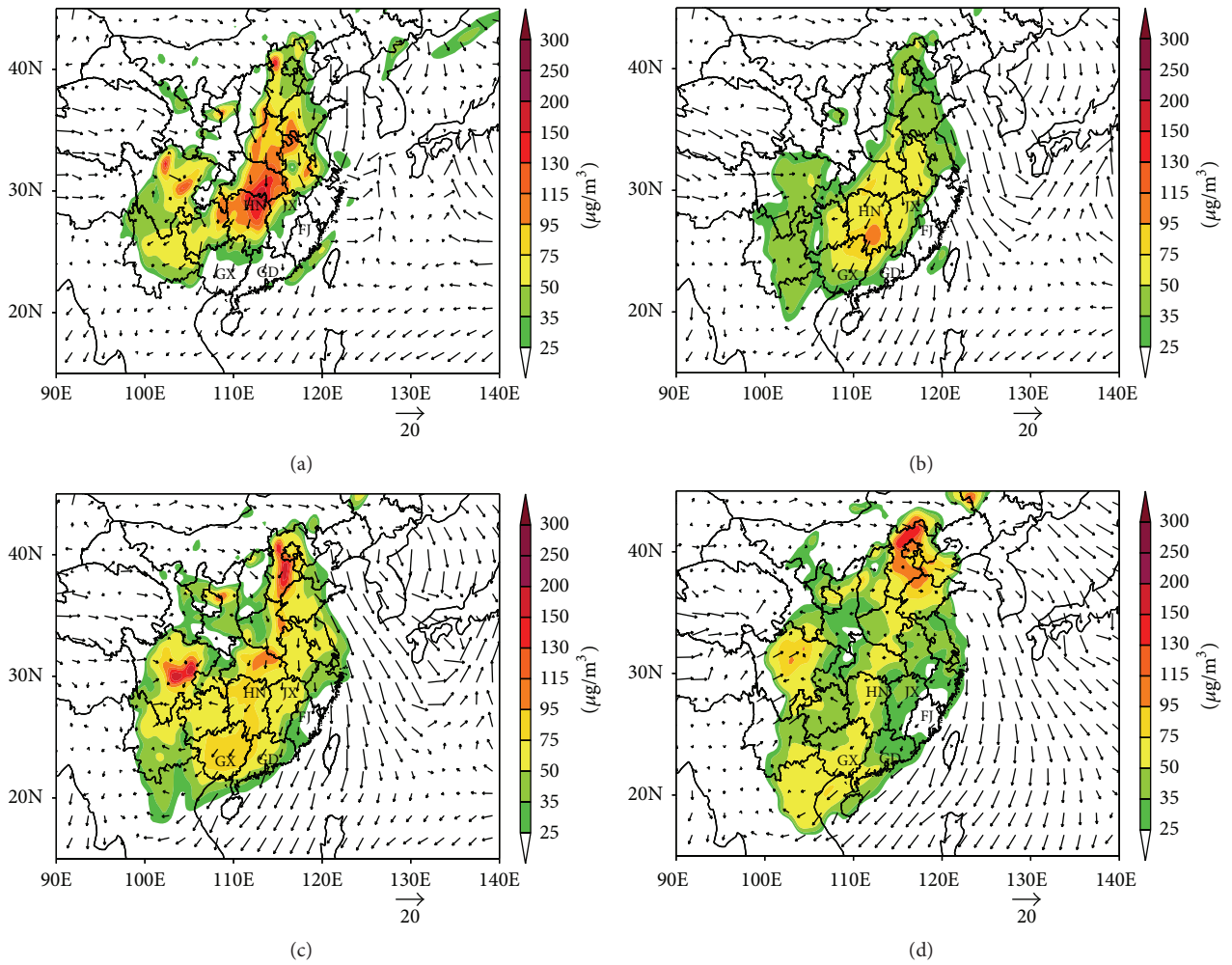

Figure 7: The spatial distribution of simulated $PM_{2.5}$ ($\mu g/m^3$) and 10 m wind fields (m/s) at (a) 08:00 LST (Local Standard Time); (b) 17:00 LST; (c) 23:00 LST on 8 January; and (d) 17:00 LST on 9 January, 2014 (the names of the provinces in the pictures: Guangdong Province (GD), Guangxi Province (GX), Hunan Province (HN), Jiangxi Province (JX), and Fujian Province (FJ)).

pollutants were transported southwards and caused large increase of $PM_{2.5}$ concentrations in northern Guangdong Province. On the night of 8 January, a large amount of pollutants was transported to the PRD region and the western part of Guangdong Province. By the afternoon of 9 January, the $PM_{2.5}$ concentrations in the PRD started to decrease. Meanwhile, $PM_{2.5}$ concentrations were decreased due to the diffusion and sedimentation. Similar transport processes of pollutants were also observed for other cases with cold front intrusions. Thus, regional transport of air pollutants from outside of Guangdong Province poses a large impact on the local haze pollution in Zhongshan during winter.

4.3. Impact of Local Emission Control on $PM_{2.5}$ at Different Time Periods. As discussed above, the emission control is the most effective in $PM_{2.5}$ reduction when there is no cold front intrusion or the regional transport is not important. The effectiveness of local emission becomes much less when there is a strong cold front intrusion. In this section, we focused on the impact of local emission control on the different stages. For this purpose, an additional simulation is completed for a single 3-day episode under no cold front condition. In this simulation, the whole emissions of Zhongshan area are turned off firstly, and then the industrial, residential, and mobile emissions of local Zhongshan are turned off one by one to evaluate their respective impact on local $PM_{2.5}$ concentrations.

Table 4 shows the changes of $PM_{2.5}$ and visibility in Zhongshan on different days when local emissions are turned off and there is no cold front intrusion. It is clear that emission control has different impact on the different days. Specifically, $PM_{2.5}$ concentrations are decreased by 47%, 52%, and 58% on the first, second, and third day, respectively, after the local emissions are turned off in Zhongshan. It is apparent that emission control has a clear phase effect. Similar phase effect is also observed for the changes of the local visibility which is increased by 57%, 63%, and 90% on the first, second, and third days, respectively. Therefore, the large impact of local emission on $PM_{2.5}$ tends to appear on the second and third day after the local emissions are turned off. This suggests that

Table 4: Percentage changes of simulated $PM_{2.5}$ concentrations and visibility after local emissions are turned off in Zhongshan.

The day after emissions are turned off	$PM_{2.5}$ concentrations (%)	Visibility (%)
1st day	−47	57
2nd day	−52	63
3rd day	−58	90

Table 5: Percentage changes of simulated $PM_{2.5}$ concentrations and visibility during heavy polluted periods after turning off industrial, residential, and mobile emissions in Zhongshan.

Emissions to be turned off	$PM_{2.5}$ (%)	Visibility (%)
Industrial emissions	−24	26
Residential emissions	−22	21
Mobile emissions	−15	16

the emission controls can be implemented on 2-3 days before a haze episode appears based on air quality forecasting.

Industrial, residential, and mobile emissions are the three major emissions to local $PM_{2.5}$ in Zhongshan given the limited impact of emissions from power plants. Now, we evaluate the impact of the three emissions on $PM_{2.5}$ in Zhongshan during a heavy haze pollution event. Here, we evaluate their impact on $PM_{2.5}$ during a peak period on the third day after the emission control is implemented. It is found from Table 5 that the industrial emission has the largest impact (−24%), the mobile emission has the smallest impact (−15%), and the residential emission stands between them when the three emissions are turned off individually. Meanwhile, the visibility is increased by 26%, 21%, and 16%, respectively. Therefore, the government should consider the optimal implementation time of the emission control in order to reduce the frequency of occurrence and severity of heavy haze events.

5. Conclusions

An offline coupling system of WRF-CMAQ is utilized to simulate $PM_{2.5}$ and to quantify the relative contribution of local emission and regional transport to the change of $PM_{2.5}$ in Zhongshan, China. Full-month simulations are performed using the WRF-CMAQ modeling system with two-nested domains for January 2014. Several numerical experiments are conducted to investigate the impact of the emissions from different regions and weather conditions on $PM_{2.5}$ and visibility in Zhongshan. Both meteorological and $PM_{2.5}$ simulations are evaluated with the surface observational data. A series of statistical parameters are used to evaluate the models' performance. The results show that the WRF provides reasonable inputs for driving CMAQ. The CMAQ is able to capture the variation patterns of $PM_{2.5}$ in Zhongshan.

The numerical sensitivity results show that the local emissions have the largest impact on $PM_{2.5}$ in Zhongshan (58%) when there is no cold front intrusion. However, the role of emissions from outside of Guangdong Province tends to be more important (52%) when a strong cold front is extended to the PRD region. The emissions from other cities in the PRD become the most important ones (42%) when a weak cold front appears.

A case study demonstrates that emission control has a clear phase accumulative effect on $PM_{2.5}$ in Zhongshan under no cold front condition. $PM_{2.5}$ concentrations of Zhongshan are decreased by 47%, 52%, and 58% on the first, second, and third day, respectively, after the local emissions are turned off. This suggests that the emission control should be implemented on 2-3 days earlier than the day when a heavy haze event happens. Finally, the sensitivity study confirms that industrial, residential, and mobile emissions are the three major sources to $PM_{2.5}$ in Zhongshan. Their relative contributions to $PM_{2.5}$ are 24%, 22%, and 15% in Zhongshan during a peak period of the sensitivity simulations.

Competing Interests

The authors declare that they have no competing interests.

Acknowledgments

This study is supported by the Key Projects in the National Science & Technology Pilar Program (2014BAC16B06), project supported by the National Natural Science Foundation of China (41205123), Science & Technology Research Project of Guangdong Meteorological Service, China (2014B32), and Special Research Project of Public Service Sectors (GYHY201306042). Also, the emission source inventory used in this paper is supplied by Center for Earth System Science from Tsinghua University, China. The authors would like to thank all people for their great work which helped to improve this paper.

References

[1] T. Wang, X. L. Wei, A. J. Ding et al., "Increasing surface ozone concentrations in the background atmosphere of Southern China, 1994–2007," *Atmospheric Chemistry and Physics*, vol. 9, no. 16, pp. 6217–6227, 2009.

[2] Y.-C. Li, J. Z. Yu, S. S. H. Ho, Z. Yuan, A. K. H. Lau, and X.-F. Huang, "Chemical characteristics of $PM_{2.5}$ and organic aerosol source analysis during cold front episodes in Hong Kong, China," *Atmospheric Research*, vol. 118, pp. 41–51, 2012.

[3] X. X. Tie, D. Wu, and G. Brasseur, "Lung cancer mortality and exposure to atmospheric aerosol particles in Guangzhou, China," *Atmospheric Environment*, vol. 43, no. 14, pp. 2375–2377, 2009.

[4] D. Wu, X. X. Tie, C. Li et al., "An extremely low visibility event over the Guangzhou region: a case study," *Atmospheric Environment*, vol. 39, no. 35, pp. 6568–6577, 2005.

[5] Q. Lu, J. Zheng, S. Ye, X. Shen, Z. Yuan, and S. Yin, "Emission trends and source characteristics of SO2, NOx, PM10 and VOCs in the Pearl River Delta region from 2000 to 2009," *Atmospheric Environment*, vol. 76, pp. 11–20, 2013.

[6] X. J. Deng, X. X. Tie, D. Wu et al., "Long-term trend of visibility and its characterizations in the Pearl River Delta (PRD) region,

China," *Atmospheric Environment*, vol. 42, no. 7, pp. 1424–1435, 2008.

[7] H. Huang, K. F. Ho, S. C. Lee et al., "Characteristics of carbonaceous aerosol in $PM_{2.5}$: Pearl Delta River Region, China," *Atmospheric Research*, vol. 104-105, pp. 227–236, 2012.

[8] P. F. Liu, C. S. Zhao, T. Göbel et al., "Hygroscopic properties of aerosol particles at high relative humidity and their diurnal variations in the North China Plain," *Atmospheric Chemistry and Physics*, vol. 11, no. 7, pp. 3479–3494, 2011.

[9] D. Wu, X. Tie, and X. Deng, "Chemical characterizations of soluble aerosols in southern China," *Chemosphere*, vol. 64, no. 5, pp. 749–757, 2006.

[10] J. H. Tan, S. J. Guo, Y. L. Ma et al., "Characteristics of particulate PAHs during a typical haze episode in Guangzhou, China," *Atmospheric Research*, vol. 102, no. 1-2, pp. 91–98, 2011.

[11] D. Wu, J. T. Mao, X. J. Deng et al., "Black carbon aerosols and their radiative properties in the Pearl River Delta region," *Science in China, Series D: Earth Sciences*, vol. 52, no. 8, pp. 1152–1163, 2009.

[12] H. J. Xu, X. M. Wang, U. Poschl et al., "Genotoxicity of total and fractionated extractable organic matters in fine air particulate matter (PM2.5) in unban Guangzhou: comparison between haze and non-haze episode days," *Environmental Toxicology and Chemistry*, vol. 27, no. 1, pp. 206–212, 2008.

[13] H. Yu, C. Wu, D. Wu, and J. Z. Yu, "Size distributions of elemental carbon and its contribution to light extinction in urban and rural locations in the pearl river delta region, China," *Atmospheric Chemistry and Physics*, vol. 10, no. 11, pp. 5107–5119, 2010.

[14] C. K. Chan and X. H. Yao, "Air pollution in mega cities in China," *Atmospheric Environment*, vol. 42, no. 1, pp. 1–42, 2008.

[15] G. S. W. Hagler, M. H. Bergin, L. G. Salmon et al., "Source areas and chemical composition of fine particulate matter in the Pearl River Delta region of China," *Atmospheric Environment*, vol. 40, no. 20, pp. 3802–3815, 2006.

[16] A. P. Kesarkar, M. Dalvi, A. Kaginalkar, and A. Ojha, "Coupling of the Weather Research and Forecasting Model with AERMOD for pollutant dispersion modeling. A case study for PM10 dispersion over Pune, India," *Atmospheric Environment*, vol. 41, no. 9, pp. 1976–1988, 2007.

[17] P. Pongkiatkul and N. T. Kim Oanh, "Assessment of potential long-range transport of particulate air pollution using trajectory modeling and monitoring data," *Atmospheric Research*, vol. 85, no. 1, pp. 3–17, 2007.

[18] W. P. Shan, Y. Q. Yin, H. X. Lu, and S. X. Liang, "A meteorological analysis of ozone episodes using HYSPLIT model and surface data," *Atmospheric Research*, vol. 93, no. 4, pp. 767–776, 2009.

[19] J.-M. Wan, M. Lin, C.-Y. Chan et al., "Change of air quality and its impact on atmospheric visibility in central-western Pearl River Delta," *Environmental Monitoring and Assessment*, vol. 172, no. 1–4, pp. 339–351, 2011.

[20] Q. Fan, J. Lan, Y. M. Liu et al., "Diagnostic analysis of the sulfate aerosol pollution in spring over Pearl River Delta, China," *Aerosol and Air Quality Research*, vol. 15, no. 1, pp. 46–57, 2015.

[21] W. Che, J. Zheng, S. Wang, L. Zhong, and A. Lau, "Assessment of motor vehicle emission control policies using Model-3/CMAQ model for the Pearl River Delta region, China," *Atmospheric Environment*, vol. 45, no. 9, pp. 1740–1751, 2011.

[22] R. Zhang, G. Sarwar, J. C. H. Fung, and A. K. H. Lau, "Role of photoexcited nitrogen dioxide chemistry on ozone formation and emission control strategy over the Pearl River Delta, China," *Atmospheric Research*, vol. 132-133, pp. 332–344, 2013.

[23] Y. R. Feng, A. Y. Wang, D. Wu, and X. D. Xu, "The influence of tropical cyclone Melor on PM_{10} concentrations during an aerosol episode over the Pearl River Delta region of China: numerical modeling versus observational analysis," *Atmospheric Environment*, vol. 41, no. 21, pp. 4349–4365, 2007.

[24] F. Jiang, T. J. Wang, T. T. Wang, M. Xie, and H. Zhao, "Numerical modeling of a continuous photochemical pollution episode in Hong Kong using WRF-chem," *Atmospheric Environment*, vol. 42, no. 38, pp. 8717–8727, 2008.

[25] X. S. Wang, Y. H. Zhang, Y. H. Hu et al., "Decoupled direct sensitivity analysis of regional ozone pollution over the Pearl River Delta during the PRIDE-PRD2004 campaign," *Atmospheric Environment*, vol. 45, no. 28, pp. 4941–4949, 2011.

[26] L. Zhong, P. K. K. Louie, J. Zheng et al., "Science-policy interplay: air quality management in the Pearl River Delta region and Hong Kong," *Atmospheric Environment*, vol. 76, pp. 3–10, 2013.

[27] H. Liu, X. M. Wang, J. M. Pang, and K. B. He, "Feasibility and difficulties of China's new air quality standard compliance: PRD case of $PM_{2.5}$ and ozone from 2010 to 2025," *Atmospheric Chemistry and Physics*, vol. 13, no. 23, pp. 12013–12027, 2013.

[28] W. C. Skamarock, J. B. Klemp, J. Dudhia, D. O. Gill, D. M. Barker, and M. G. Duda, "A description of the advanced research WRF version 3," NCAR Technical Note NCAR/TN-475+STR, 2008.

[29] S. Y. Hong and J. O. J. Lim, "The WRF single-moment 6-class microphysics Scheme (WSM6)," *Journal of the Korean Meteorological Society*, vol. 42, no. 2, pp. 129–151, 2006.

[30] D. L. Zhang and R. A. Anthes, "A high-resolution model of the planetary boundary layer—sensitivity tests and comparisons with SESAME-79 data," *Journal of Applied Meteorology*, vol. 21, no. 11, pp. 1594–1609, 1982.

[31] F. Chen and J. Dudhia, "Coupling and advanced land surface-hydrology model with the Penn State-NCAR MM5 modeling system. Part I: model implementation and sensitivity," *Monthly Weather Review*, vol. 129, no. 4, pp. 569–585, 2001.

[32] S.-Y. Hong, Y. Noh, and J. Dudhia, "A new vertical diffusion package with an explicit treatment of entrainment processes," *Monthly Weather Review*, vol. 134, no. 9, pp. 2318–2341, 2006.

[33] G. Sarwar, D. Luecken, G. Yarwood, G. Z. Whitten, and W. P. L. Carter, "Impact of an updated carbon bond mechanism on predictions from the CMAQ modeling system: preliminary assessment," *Journal of Applied Meteorology & Climatology*, vol. 47, no. 1, pp. 3–14, 2008.

[34] W. T. Hutzell, D. J. Luecken, K. W. Appel, and W. P. L. Carter, "Interpreting predictions from the SAPRC07 mechanism based on regional and continental simulations," *Atmospheric Environment*, vol. 46, pp. 417–429, 2012.

[35] Q. Zhang, D. G. Streets, G. R. Carmichael et al., "Asian emissions in 2006 for the NASA INTEX-B mission," *Atmospheric Chemistry and Physics*, vol. 9, no. 14, pp. 5131–5153, 2009.

[36] Q. Zhang, G. N. Geng, S. W. Wang, A. Richter, and K. B. He, "Satellite remote sensing of changes in NO_x emissions over China during 1996–2010," *Chinese Science Bulletin*, vol. 57, no. 22, pp. 2857–2864, 2012.

[37] K. B. He, "Multi-resolution Emission Inventory for China (MEIC): model framework and 1990–30 2010 anthropogenic emissions," in *Proceedings of the International Global Atmospheric Chemistry Conference*, 1990.

[38] J.-Y. Zheng, Z.-Y. Zheng, Z.-L. Wang, L.-J. Zhong, and D. Wu, "Biogenic VOCs emission inventory and its temporal and

spatial characteristics in the Pearl River Delta area," *China Environmental Science*, vol. 29, no. 4, pp. 345–350, 2009.

[39] L. T. Wang, J. M. Hao, K. B. He et al., "A modeling study of coarse particulate matter pollution in Beijing: regional source contributions and control implications for the 2008 Summer Olympics," *Journal of the Air and Waste Management Association*, vol. 58, no. 8, pp. 1057–1069, 2008.

[40] J. Xing, Y. Zhang, S. X. Wang et al., "Modeling study on the air quality impacts from emission reductions and atypical meteorological conditions during the 2008 Beijing Olympics," *Atmospheric Environment*, vol. 45, no. 10, pp. 1786–1798, 2011.

[41] J. F. Sisler and W. C. Malm, "Interpretation of trends of $PM_{2.5}$ and reconstructed visibility from the IMPROVE network," *Journal of the Air & Waste Management Association*, vol. 50, no. 5, pp. 775–789, 2000.